

# Gauges for fine and high vacuum

*K. Jousten*

Physikalisch-Technische Bundesanstalt, 10587 Berlin, Germany

## Abstract

Vacuum gauges for use in accelerators have to cover about 17 decades of pressure, from  $10^{-12}$  Pa to  $10^5$  Pa. In this article we describe the history, measurement mode, design, accuracy and calibration of the gauges used down to  $10^{-5}$  Pa. We focus on commercially available types of gauges, i.e., mechanical gauges, piezoresistive and capacitance diaphragm gauges, thermal conductivity gauges, and spinning rotor gauges.

## 1 Introduction

For about 350 years, from 1644 to about 1900, the Torricelli tube was the only instrument able to measure vacuum. It was based on the counterbalance of the gravitational force of a mercury column against a pressure difference in two volumes separated by the liquid mercury. If one of the volumes was under ‘vacuum’ conditions (i.e., the mercury vapour pressure), it was an absolute instrument and pressure was measured in ‘mmHg’ and later in ‘Torr’.

Unfortunately these units are still being used today in some areas, even though the Torricelli tube is out of practical use and the Metre Convention (CGPM) was implemented almost 50 years ago in 1960 when the *Système International* (SI) of physical units replaced the Torr by the pascal. The pascal (Pa) is the force of 1 newton on  $1\text{ m}^2$  as pressure is defined by

$$p = F/A . \quad (1)$$

One can still use the bar for  $10^5$  Pa, hence 1 mbar is equal to 100 Pa. In this article we shall use mainly the unit Pa.

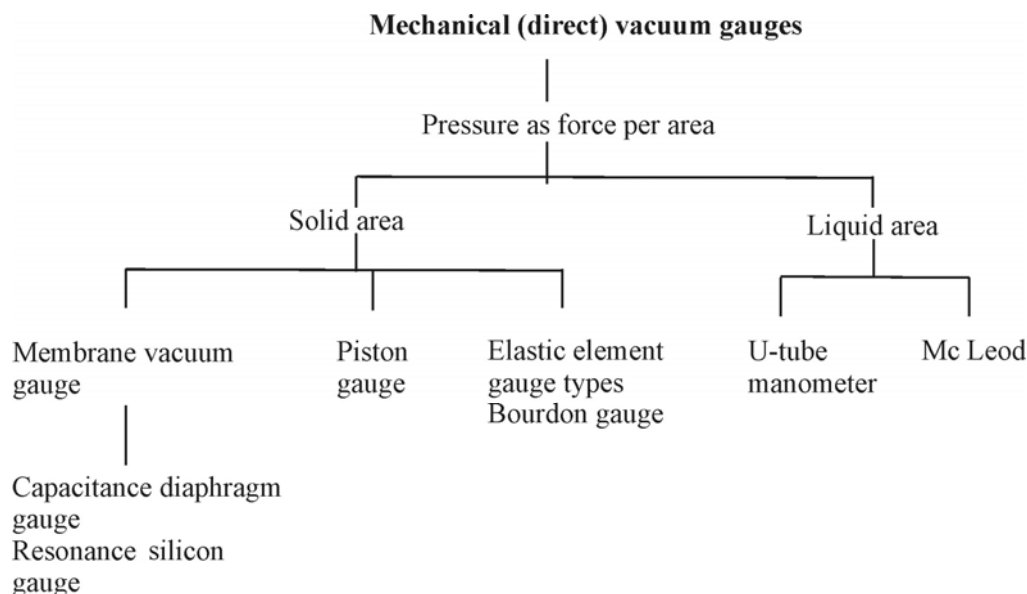
The measurement of vacuum pressure follows Eq. (1)

- by a direct measurement of the force per area (direct gauges)
- or indirectly by measurement of a quantity that is proportional to pressure, e.g., the molecular density, the impingement rate of molecules, the thermal conductivity, etc.

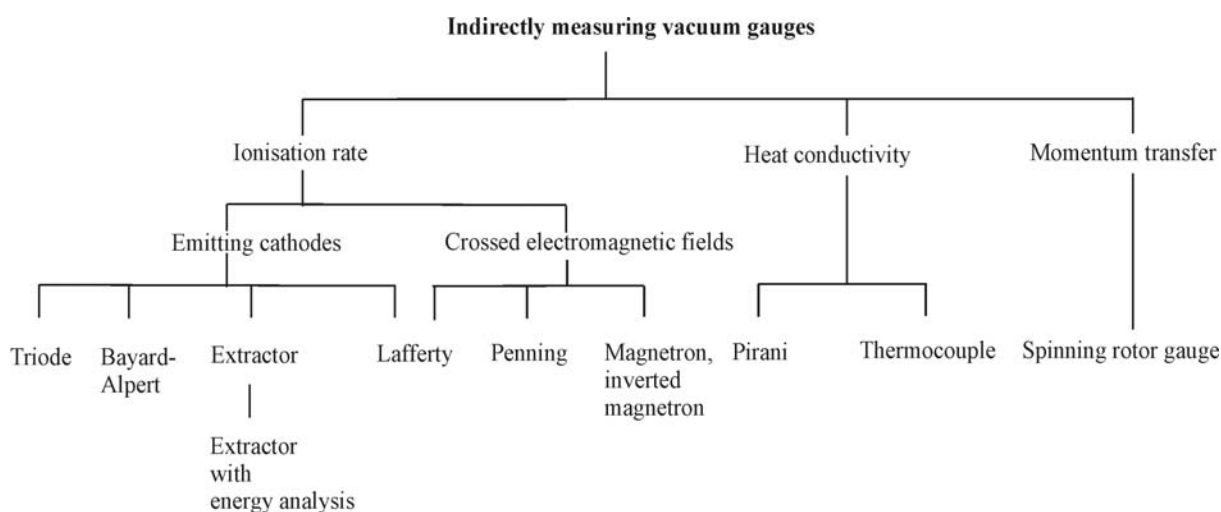
The direct measurement of pressure is limited to pressures larger than about 1 mPa. At this pressure, the force on  $1\text{ cm}^2$  is only  $10^{-7}$  N which already needs an electrically amplified signal.

Figure 1 gives a classification scheme of vacuum gauges measuring pressure directly, Fig. 2 gives the most well-known types of vacuum gauges measuring pressure indirectly by another quantity.

The direct measuring vacuum gauges have the great advantage that their reading is independent of the gas species. They truly measure a total pressure of a gas mixture or a pure gas. The signal of indirect measuring vacuum gauges, on the other hand, depends for a given pressure on the gas species and for this reason it may not be possible to convert the signal into a correct pressure reading if the gas composition of a mixture is not known exactly.



**Fig. 1:** Classification of directly measuring vacuum gauges



**Fig. 2:** Classification of indirectly measuring vacuum gauges according to their principle of measurement

Before we go into any details of vacuum measurement, let us say a word that is true for any measurement device. To measure something always means to compare a quantity with a unit for this quantity. The unit is internationally defined and realized in National Metrological Institutes and further disseminated to calibration laboratories and manufacturers and users of measuring equipment. It is hoped that each measuring instrument is somehow traceable to a so-called primary standard for this unit. This can be visualized by the pyramid of the calibration chain (Fig. 3). On each level some accuracy is lost. In the case of vacuum gauging there are several National Institutes that realize the pressure scale for vacuum pressures, which are published on the Web site of the BIPM [1], the Bureau International des Poids et Mesures.

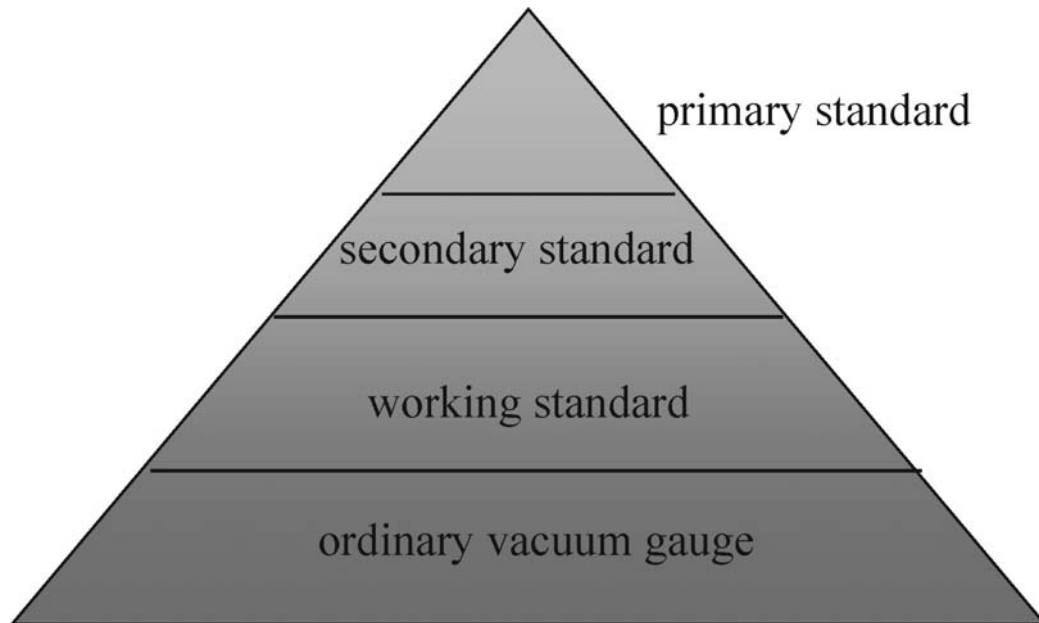


**Fig. 3:** The pyramid of the calibration chain. On each level downwards some information and accuracy are lost

One should also note the distinction between error and uncertainty of a measurement device. An error of the reading of a measurement device is the difference of the measured value from the true value of the quantity as defined by the SI system. After errors have been removed and all corrections known were made, still, each determined value of a physical quantity is an estimation. The uncertainty of a measured value gives the possible range by which the reading may not reflect the true value defined by the SI unit (Fig. 4). A high quality measurement will give a low uncertainty and vice versa. Without the concept of uncertainty, measured values cannot be compared, either among themselves or with reference values obtained somewhere else. Every measured value must be accompanied by its uncertainty in order to achieve comparability in a community.

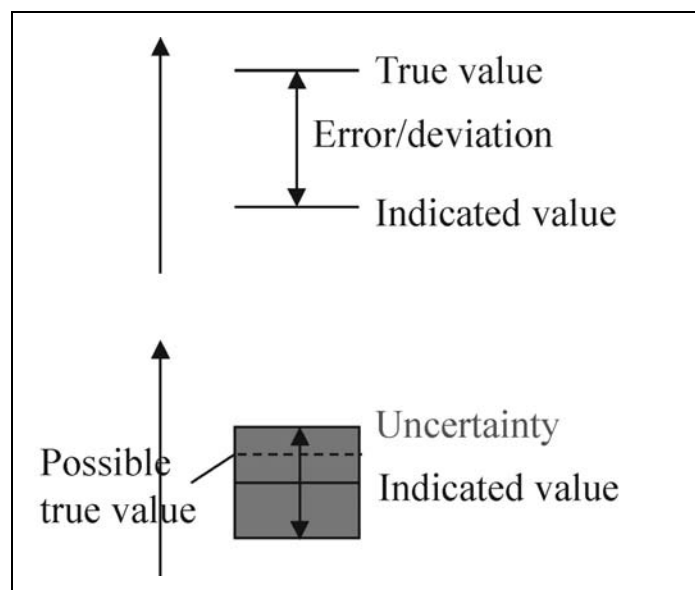


**Fig. 4:** The concept of error and uncertainty

## 2 Direct measuring vacuum gauges

### 2.1 Mercury manometer and the McLeod gauge

The mercury manometer (Fig. 5) is still the most accurate pressure gauge when operated carefully. Owing to the hazard of mercury it has almost disappeared from the commercial market, but it is used by the National Metrological Institutes where highest accuracy is required.

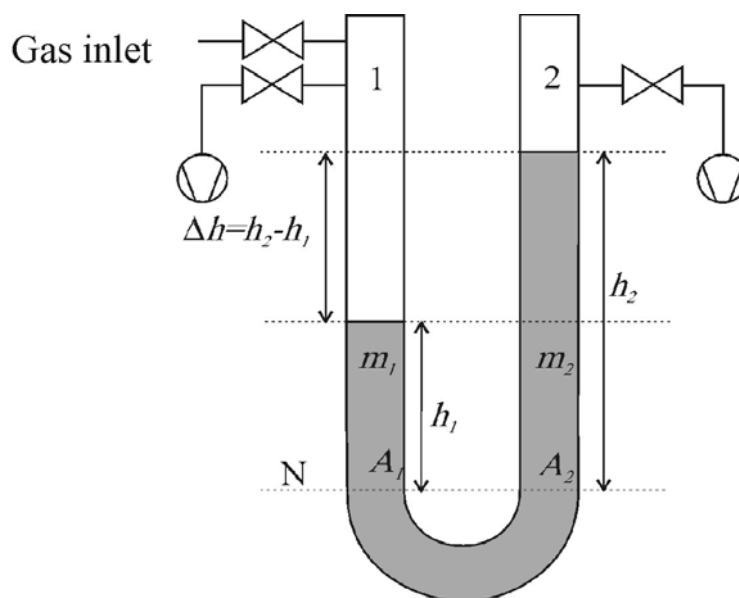


**Fig. 5:** The principal measurement scheme of the mercury manometer

The pressure difference between the two volumes 1 and 2 (Fig. 5) is given by

$$p_1 - p_2 = \rho g \Delta h \quad (2)$$

where  $\rho$  is the well-known density of mercury,  $g$  the local acceleration due to gravity. Volume 2 is usually pumped down to the fine vacuum and  $p_2$  is approximately given by the vapour pressure of mercury. Since both  $\rho$  and  $g$  can be determined with high accuracy and  $\Delta h$  can also be determined with very low uncertainty by either optical interferometrical methods [2], [3] or phase-sensitive ultrasound detection [4],  $p_1$  can be measured with the highest accuracy (relative uncertainties can be as low as  $2 \cdot 10^{-6}$ ).

Mercury manometers are the primary standards for vacuum pressures from about 100 Pa to  $10^5$  Pa and therefore the traceability of pressure to the SI units of mass, time, and length.

Of historical importance is also the so-called McLeod gauge, which allowed the range of the mercury U-tube to be extended by several orders of magnitude by compressing the gas to be measured by moving the mercury in capillaries. It was invented in 1873 by H.G. McLeod and served as primary standard for pressures from  $10^{-4}$  Pa up to the range of the mercury manometer until the 1960s.

### 2.2 Piston gauges

Figure 6 shows the principal measurement scheme of a rotating piston gauge. A cylindrical piston rotates in a closely fitted circular cylinder. The pressure at the base of the piston is defined as the ratio of the total downwards force on the piston to the effective area of the piston-cylinder assembly when floating at its operating level.

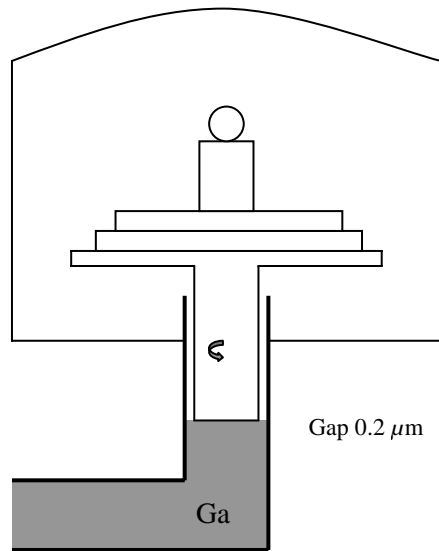


**Fig. 6:** The principal measurement scheme of a rotating piston gauge

The rotating piston gauge is a pressure generator, since the piston will float only when the pressure underneath exactly cancels the force from the top that may be varied by weights put on the piston. The pressure in the evacuated bell jar must be considered for absolute pressure measurement as volume 2 (Fig. 5) in the mercury manometer. The gap between piston and cylinder is typically a few tenths of a micron at a cross-section of  $10 \text{ cm}^2$ .

The rotation of the piston is needed to avoid any friction effects. Piston gauges can serve as primary standards for vacuum with somewhat higher uncertainty than mercury manometers from  $10^3 \text{ Pa}$  up to atmospheric pressure.

Non-rotating piston-cylinder assemblies are also used. In that case a balance is used to measure the force  $F$ , and the effective area  $A$  is determined by calibration with a mercury manometer (Fig. 7). These gauges have a resolution down to  $1 \text{ mPa}$  and have a good accuracy from  $10 \text{ Pa}$  up to about  $10 \text{ kPa}$  which is their upper pressure limit.

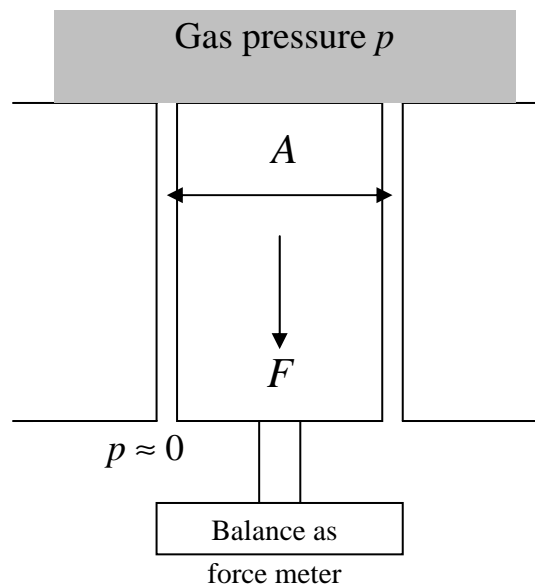


**Fig. 7:** The principal measurement scheme of a pressure balance

### 2.3 Mechanical gauges

Most mechanical gauges use a membrane to detect the force of the pressure (Fig. 8). On this membrane the force

$$F = (p_1 - p_2)A \quad (3)$$

is exerted, which will cause a deflection  $x$  of the membrane that can be used for measurement. In most cases  $x$  is converted into an angle  $\varphi$  that can be used for a needle indicator (see Fig. 8). When the reference pressure  $p_2$  is negligible compared to  $p_1$  the instrument shows the absolute pressure. Most common mechanical vacuum meters can be classified in three groups.

- The reference pressure is the prevailing atmospheric pressure. The measurement device is located on the reference side (a).
- The reference pressure is zero. The measurement device is located on the other (test) side (b).
- The reference pressure is zero. The measurement device is located on the same reference side (c).

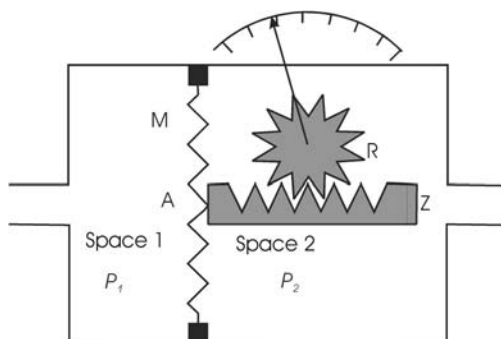


**Fig. 8:** The measurement scheme of a membrane gauge. From *Wutz Handbuch Vakuumtechnik* by K. Jousten (ed.), Vieweg Verlag.

An example of the latter type is shown in Fig. 9. This type has the advantage that the gas to be measured is not in contact with the sensitive instrumentation. The gauge is more resistant against corrosion. Only the membrane bellows normally made of a copper–beryllium alloy have to be protected against corrosive gases.

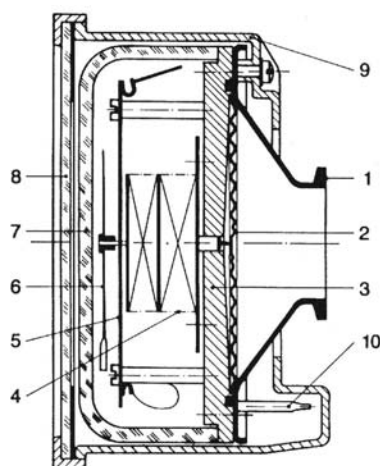


**Fig. 9:** Schematic of a membrane gauge with mechanical reading. 1 connecting flange; 2 membrane; 3 ground plate; 4 indicating system of membrane deformation; 5 indicating scale; 6 needle pointer; 7 glass vacuum enclosure; 8, 9 housing; 10 evacuation stem. From *Wutz Handbuch Vakuumtechnik* by K. Jousten (ed.), Vieweg Verlag.

A common example of type (a) is the so-called Bourdon gauge. Here a bent tube with a normally elliptical cross-section is closed at one end, and open to the gas to be measured at the other end. When the pressure inside the tube changes, the radius of curvature changes, since the force change on the outer side of the tube will be smaller due to the larger area than on the inner side of the bended tube. The bending is transformed by a lever to a needle pointer. The disadvantage of this type of cheap and robust gauge is that the reading depends on the atmospheric pressure. This can be corrected by turning the scale against the pointer.

#### 2.4 Direct gauges with electrical output

The Bourdon gauge was greatly refined by the Quartz Bourdon Spiral (QBS) gauge (Fig. 10). A quartz helix is used as a tube. The bending of the helix is compensated by a force exerted by two electromagnetic coils. The balancing current through the coils is proportional to pressure. The null position is sensed optically via a mirror on the free end of the helix which reflects a beam light detected by two photocells. Since the helix remains fixed, hysteresis effects are negligible and the device can be linearized very well. The relative measurement uncertainty is in the low  $10^{-4}$  range near full scales available from 7 kPa up to a few 100 kPa. The lowest reasonably measurable pressure is about 1 kPa.

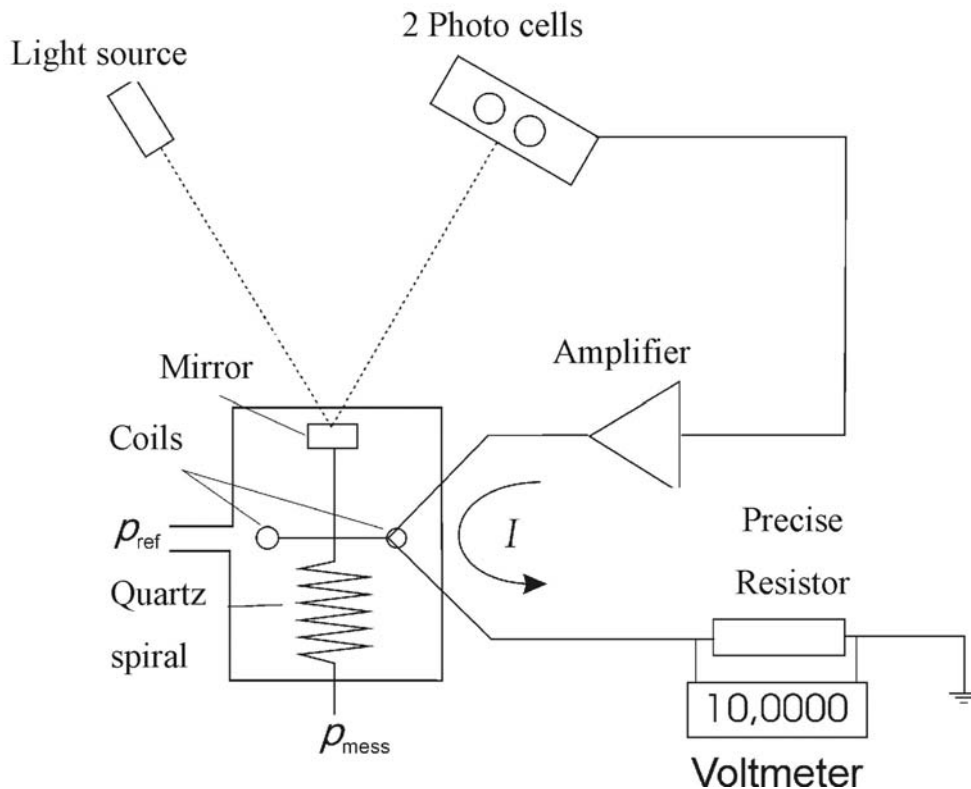


**Fig. 10:** Schematic of a Quartz Bourdon Spiral by Ruska, Houston, Texas. From *Wutz Handbuch Vakuumtechnik* by K. Jousten (ed.), Vieweg Verlag.

Another gauge of type (c) is the piezo-electrical vacuum meter (Fig. 11). A force on a quartz crystal generates a charge at the surface which may be measured by an electrometer. Since a pressure acting on all sides of a crystal will not do the job, a membrane is used that generates a force acting on one end of a quartz beam only. The generated charge is then guided to the electrical connector to the electrometer.

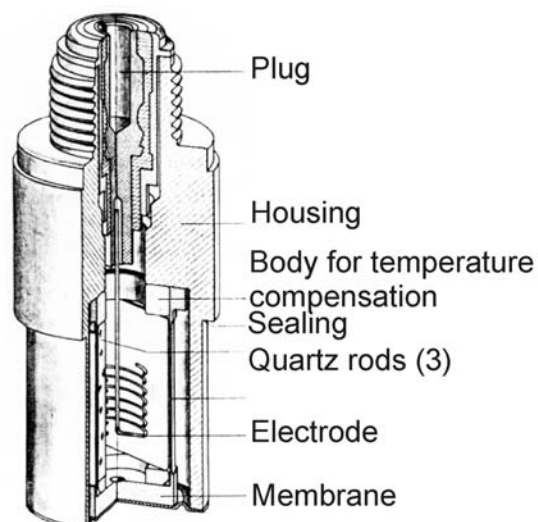


**Fig. 11:** Design of a piezo-electrical vacuum gauge

Other membrane gauges use the piezo-resistive effect to detect the force acting on the membrane (Fig. 12). In this effect the resistance is changed by a geometrical change of the material and for semiconductors, in addition, by a change of the specific resistance. Therefore mainly semiconductor materials are used for this type of gauge. A silicon crystal that has excellent elastic behaviour is used as the membrane. The low-ohmic resistive ‘wires’ are obtained by doting the silicon in two directions of the membrane. The resistors are part of a bridge circuit. A compensation for temperature effects has to be provided.

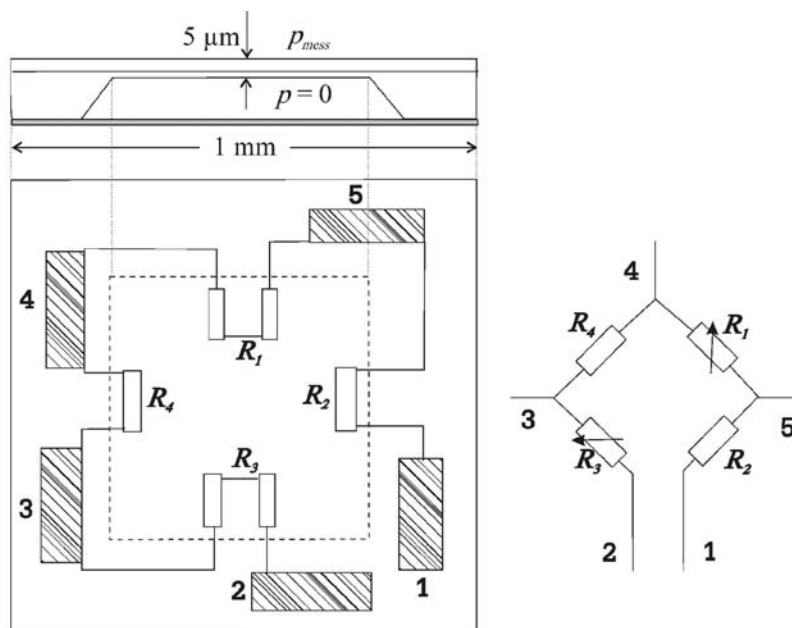


**Fig. 12:** Schematic diagram of a piezo-resistive vacuum gauge. The device is MEMS fabricated on silicon. From *Wutz Handbuch Vakuumtechnik* by K. Jousten (ed.), Vieweg Verlag.

In the capacitance diaphragm gauge (CDG) the membrane is used as one electrode of a capacitor (Fig. 13). When the membrane is deflected, the capacity will change and this change is converted into the measurement signal. Since capacity can be measured with very high accuracy, it is possible to measure deflections of the membrane of 0.4 nm. This resolution limit corresponds to about 1 mPa.



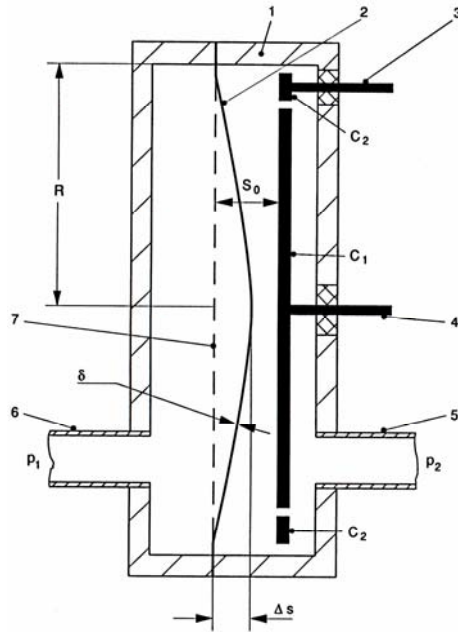


**Fig. 13:** Schematic diagram of the capacitance diaphragm gauge. 1 housing; 2 membrane; 3,4 electrical feedthroughs to capacitors; 5 gas inlet (reference side); 6 gas inlet (test side); 7 membrane in zero position. From *Wutz Handbuch Vakuumtechnik* by K. Jousten (ed.), Vieweg Verlag.

Such a good resolution and accuracy have been obtained by know-how that has been developed since 1949, mainly by the MKS company [5]. The circular membrane is manufactured from a material with very low expansion coefficient, namely the metal alloy INVAR, or ceramic. The membrane may be as thin as  $25 \mu\text{m}$ . It is welded, soldered or glued to the housing. To improve zero stability, on the reference side there are two electrodes, a circular one in the centre, and a ring electrode around, forming two capacitors. The differences of the two capacities are used as measurand. Both capacitors are part of a bridge (Fig. 14). An oscillator sends a fixed signal of a frequency of about 10 kHz to the bridge which modifies it by amplitude and phase. The amplitude is proportional to pressure, the phase gives the direction of pressure. After demodulation with the oscillator signal a DC signal is produced which is linearized and amplified [5].

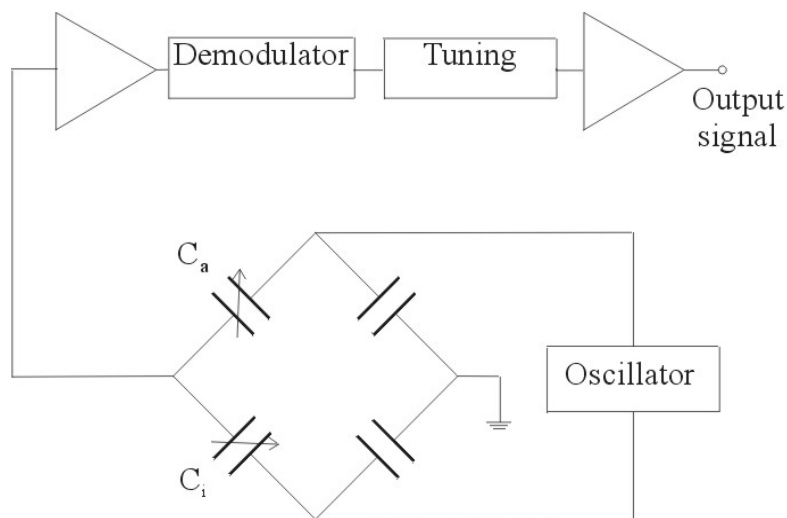


**Fig. 14:** The electrical circuit of a capacitance diaphragm gauge.  $C_i$  is the capacity between membrane and inner electrode,  $C_a$  between membrane and outer ring electrode (Fig. 13). From *Wutz Handbuch Vakuumtechnik* by K. Jousten (ed.), Vieweg Verlag.

Since this instrument is so sensitive, temperature drifts may cause a large change of the null signal. For this reason CDGs for highest accuracy are stabilized to a temperature of about 45°C with a stability of a few millikelvin. This higher temperature causes at lower pressures (< 100 Pa) the so-called thermal transpiration effect which will be treated below.

CDGs are available with both sides of the membrane accessible from the outside (differential mode) or with the reference side enclosed and pumped with a getter material (absolute mode). Their full scales range from 0.1 Torr (13 Pa) to 1000 Torr (133 kPa), their resolution varies from 3½ digits to 5½ digits. The gauge head is normally separated from the controller, but also so-called ‘active’ gauges are available which have an analog voltage output to be measured with a DVM. They are very common in the semiconductor industry and in calibration laboratories or wherever high accuracy is required.

A MEMS fabricated version of a vacuum gauge with a membrane was presented in the late 1990s [6], the so-called resonance silicon gauge (Fig. 15). Here two ‘H’-shaped resonators similar to tuning forks are fixed to a thin membrane of a Si crystal. When the membrane deflects, the eigenfrequency of the resonators is changed and a frequency signal is detuned. The resonator at the edge will reduce its frequency  $f_2$ , while the one in the centre will increase the frequency  $f_1$ . The difference ( $f_1 - f_2$ ) is proportional to pressure, the sum ( $f_1 + f_2$ ) reflects the common line pressure. Both ‘H’ resonators have to have their own vacuum enclosure, since otherwise the surrounding pressure would deteriorate the  $Q$  factor and also detune the frequency. With this casing only the deflection of the membrane causes the measurement signal. The measurement range of these gauges is at very low uncertainty ( $10^{-4}$  range) from 100 Pa to 100 kPa.

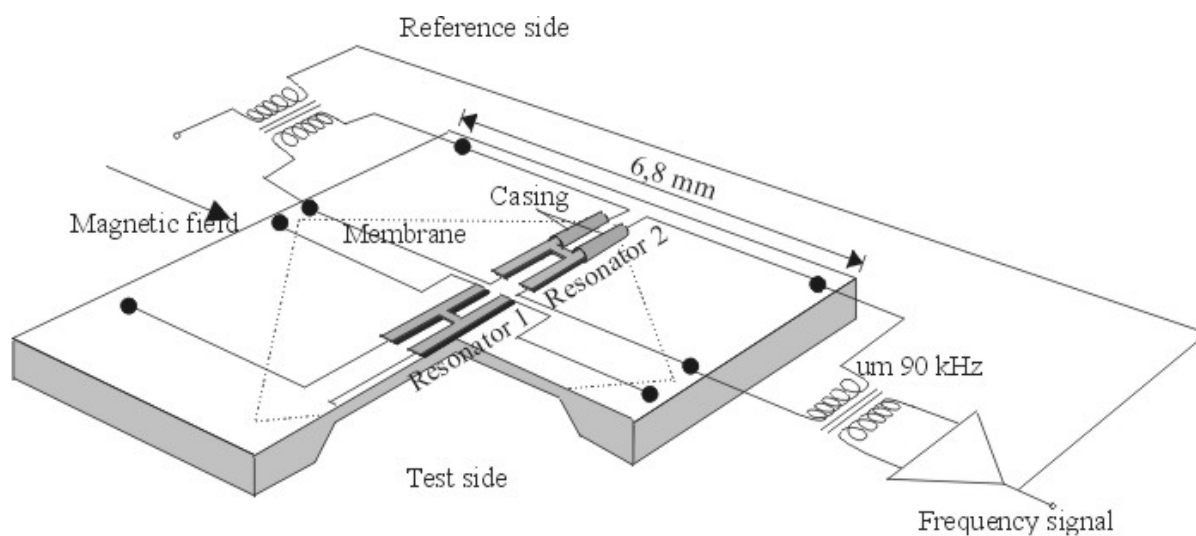


**Fig. 15:** Design of the resonance silicon gauge by Yokogawa Co, Japan. From *Wutz Handbuch Vakuumtechnik* by K. Jousten (ed.), Vieweg Verlag.

At the end of this section we would like to mention the thermal transpiration effect, since it is important for CDGs and in general for vacuum measurements. This effect develops when the pressure has dropped into the transition regime between viscous and molecular flow and when different temperatures on different locations of a vacuum system prevail (Fig. 16). In equilibrium of molecular flow, the same number of molecules must enter the left volume (Fig. 16) as leave it. Since the velocities of molecules is proportional to the square root of the temperature, this means that the molecular density must be lower when the temperature is higher. Because of the ideal gas law,  $p = nkT$ , the effect on pressure is reversed. The formulas are given on Fig. 16.

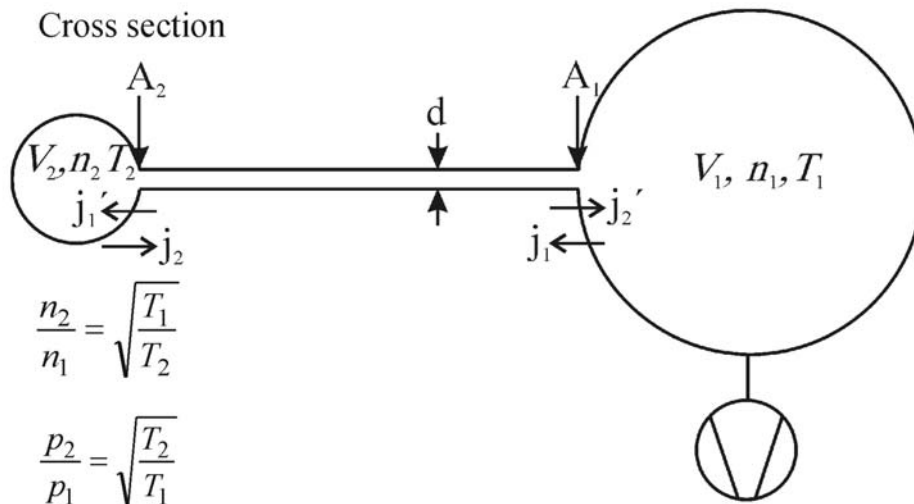


**Fig. 16:** Illustration of the effect of thermal transpiration. Two volumina of different temperature are connected together where the Knudsen number is  $> 0.5$ . From *Wutz Handbuch Vakuumtechnik* by K. Jousten (ed.), Vieweg Verlag.

Since the temperature in the CDG is about  $45^\circ\text{C}$ , the pressure in the gauge is increased by about

$$\sqrt{318/296} = 1.036 .$$

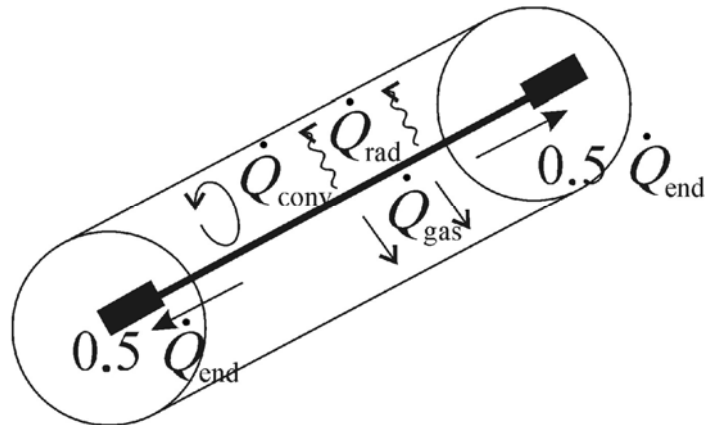
When CDGs are calibrated, this effect can clearly be seen. Both in the viscous flow regime and the molecular regime the error for the reading is constant with a transitional behaviour in between. Since the mean free path of helium extends to higher values, also the transition regime is shifted to higher pressures. The curve may be fitted accordingly [7], [8].

### 3 Indirect measuring vacuum gauges

#### 3.1 Thermal conductivity gauges

In a certain pressure range gas conducts thermal energy proportionally to the number of molecules involved in the transport. This effect can be used to measure vacuum pressures: the power (heat) loss of a heated element, usually a wire, to an enclosure of stable temperature ('room' temperature) is measured. At higher pressures the gas density is so high and the mean free path of the molecules so short that the gas can be described as a continuum. In this case there is also a heat flow from an element at higher temperature to a wall of lower temperature, but this heat flow does not depend on the pressure. At lower pressures, however, where each molecule can freely travel from the heated element to the wall, each molecule transports some energy and the total amount of energy transport is proportional to the number of molecules. In the intermediate regime the proportionality becomes weaker.

Figure 17 shows the heat flows in a thermal conductivity gauge. The desired heat flow for measurement is  $\dot{Q}_{\text{gas}}$ , which is the heat transported by the gas molecules from the heated wire to the housing. A pressure-independent null signal gives  $\dot{Q}_{\text{rad}}$ , the loss due to radiation, and  $\dot{Q}_{\text{end}}$ , the thermal conduction from the wire to its support structure. There is also some convection  $\dot{Q}_{\text{conv}}$  in the viscous flow regime. This is a disturbing effect since it is not stable and orientation dependent, but some gauges use this effect to extend the measurement range up to atmospheric pressure.



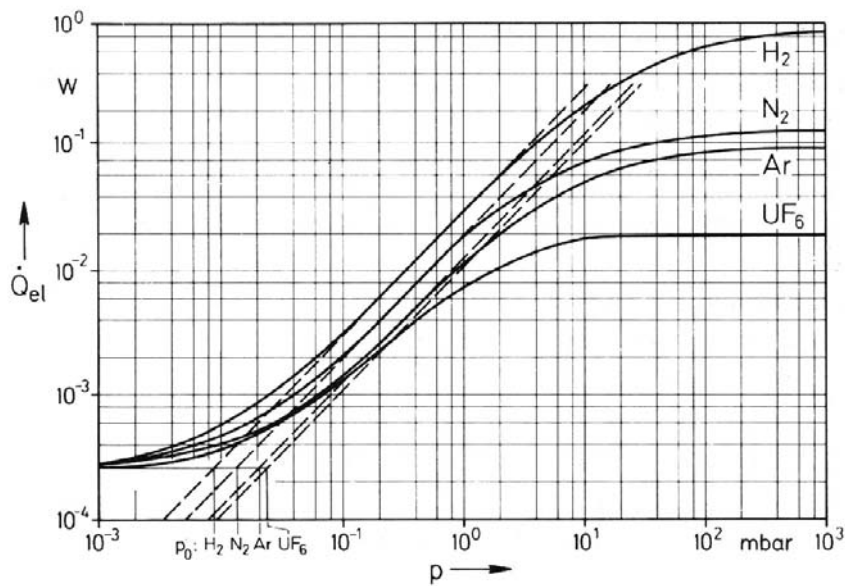
**Fig. 17:** The heat flow from a heated wire in a thermal conductivity gauge.  $\dot{Q}_{gas}$  desired heat flow by the gas molecules.  $\dot{Q}_{rad}$  heat flow by radiation.  $\dot{Q}_{conv}$  heat flow by convection.  $\dot{Q}_{end}$  thermal conduction in the wire to the holder.

Figure 18 shows the electrical power  $\dot{Q}_{el}$  needed to keep the wire temperature constant in a thermal conductivity gauge dependent on pressure. At the very low end there is the pressure independent signal due to  $\dot{Q}_{rad}$  and  $\dot{Q}_{end}$ , then  $\dot{Q}_{gas}$  dominates, and finally only convection causes a pressure-dependent signal. Neglecting the convection, we can write

$$\dot{Q}_{el} = \dot{Q}_{gas} + \dot{Q}_{end} + \dot{Q}_{rad} \tag{4}$$

which can be approximated by the following formula:

$$\dot{Q}_{el} = \varepsilon \left( p_0 + \frac{p}{1 + gp} \right) \tag{5}$$



**Fig. 18:** The electrical power needed to keep the wire temperature constant in a Pirani gauge for different gas species. From *Wutz Handbuch Vakuumentchnik* by K. Jousten (ed.), Vieweg Verlag.

If one keeps the temperature of the wire constant and measures the electrical power  $Q_{el}$  needed for this, in some pressure regime  $\dot{Q}_{el}$  will be proportional to  $p$ .

This type of gauge was invented in 1906 by Pirani [9]. He put the heated wire as part of a Wheatstone bridge which supplied the necessary electrical power. This is still done today and it is common to call a thermal conductivity gauge with a Wheatstone bridge a Pirani gauge. There are, however, several different operational modes: gauges where the temperature of the heated element is held constant are the most accurate ones with the largest measurement range, but also the most expensive. Alternatively, the heating voltage, current, or power can be kept constant (the latter was, what Penning did) and the temperature (resistance) of the wire is measured.

The electrical circuit of a Pirani gauge to keep the wire temperature constant is shown in Fig. 19. The wire has a diameter of  $10\mu\text{m}$  or less. The resistances  $R_2, R_3, R_4, R_D$ , are of about the same value.  $R_T$  is used to compensate temperature changes of the surrounding enclosure.

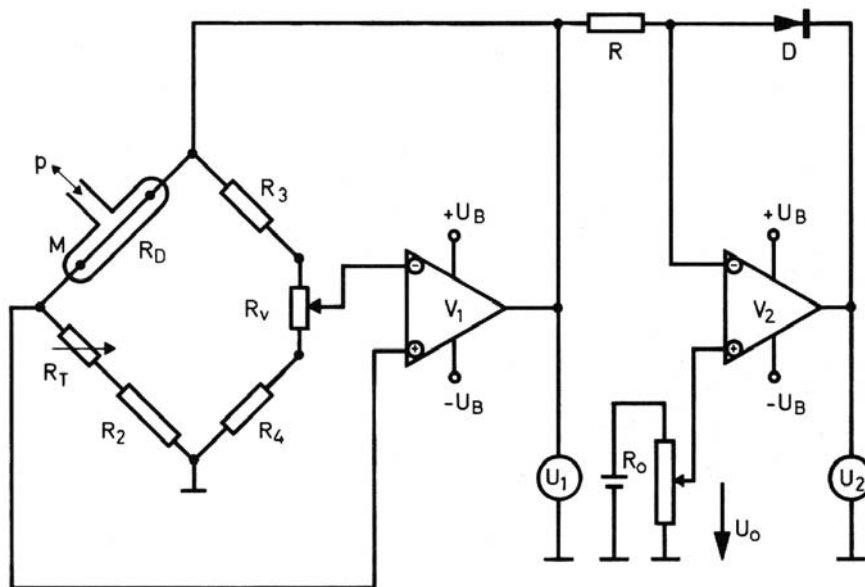


**Fig. 19:** Electrical circuit of a Pirani gauge.  $M$  measuring cell;  $R_D$  resistance of heated wire. From *Wutz Handbuch Vakuumtechnik* by K. Jousten (ed.), Vieweg Verlag.

A feature of Pirani gauges with constant temperature that may be important for accelerators is that they react faster with pressure changes, since no thermal relaxation times will cause delays which is the case in other configurations.

Most commercially available Pirani gauges need to be adjusted at atmospheric pressure and at a pressure below the resolution limit of about 10 mPa. The adjustment has to be repeated when the wire has changed (blackening, deposits etc.). Their measurement range is typically from 0.1 Pa to  $10^4$  Pa, sometimes up to atmospheric pressure.

Recently Pirani gauges have been produced by MEMS (Fig. 20). Instead of a heated wire, a heated sheet is used. The temperature was reduced to about  $60^\circ\text{C}$ , where macroscopic wires are normally at  $120^\circ\text{C}$ . A lower temperature will give a smaller null signal due to radiation and conduction, but increase the dependence on the environmental temperature changes. The small sizes by MEMS have the advantage that the Knudsen number is increased at the same pressure and therefore the molecular regime so that it can be expected that the reading will be more linear up to higher pressures. Another advantage of small structures is that no convection whirls can develop, so the gauge reading is independent of its orientation.

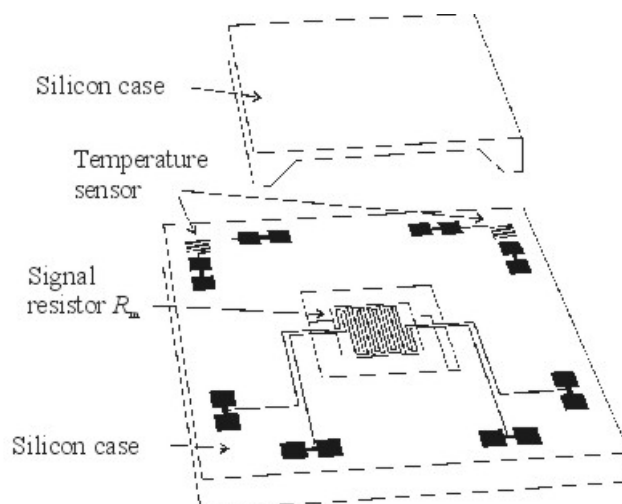


**Fig. 20:** MicroPirani of MKS produced with MEMS. Instead of a heated wire there is a heated slab. From *Wutz Handbuch Vakuumtechnik* by K. Jousten (ed.), Vieweg Verlag.

The reading of thermal conductivity gauges strongly depends on the gas species as could already be seen on Fig. 18. The physical parameters for this dependence are due to properties of the gas itself (like degrees of freedom, mean thermal velocity of the molecules), but also due to the accommodation of the gas molecules on the respective surfaces. These accommodation coefficients clearly depend on the surfaces and for this reason thermal conductivity gauges are very sensitive to any pollution.

General correction factors from text books for different gas species in thermal conductivity gauges should be handled with great care. Owing to the facts described above, the gas dependence is due to the specific surfaces involved and there is no such general value for a gas species in Pirani gauges. It can be seen from Fig. 21 that the values of different gauges scatter significantly and are also dependent on pressure.

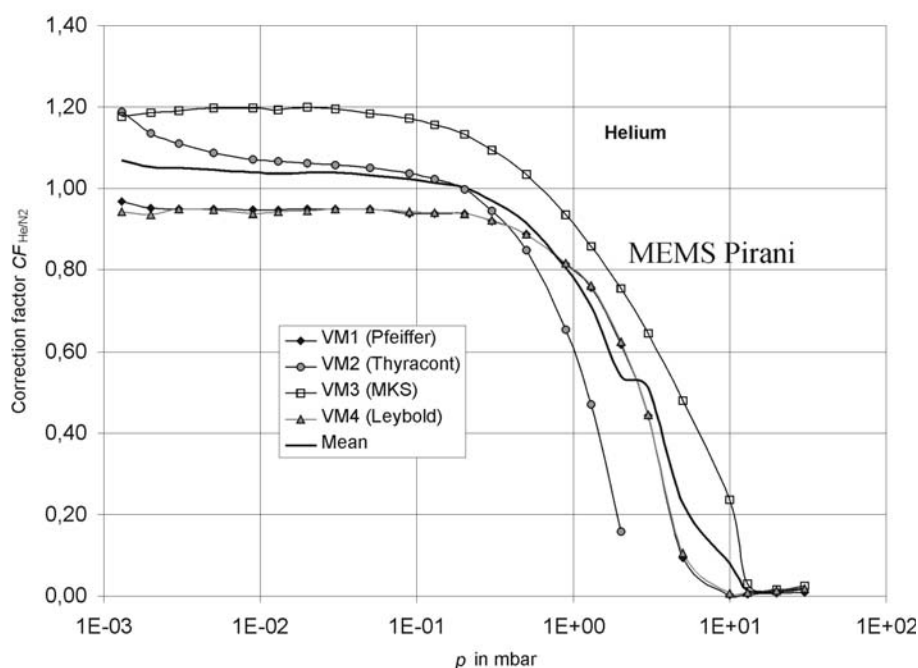


**Fig. 21:** Correction factor for helium compared to a reading for nitrogen for four different Pirani gauges vs. pressure

A very simple and cheap thermal conductivity gauge is the so-called thermocouple (Fig. 22). A constant current of typically 150 mA is sent through the heated wire and its temperature is measured by a thermocouple of chromel/alumel. The measurement range is rather limited (0.1 Pa–100 Pa) as well as the accuracy.

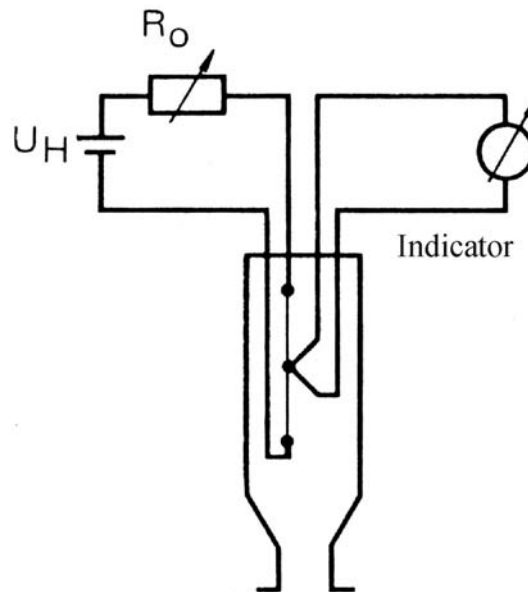


**Fig. 22:** Design of a thermocouple gauge. From *Wutz Handbuch Vakuumtechnik* by K. Jousten (ed.), Vieweg Verlag.

### 3.2 Spinning rotor gauge

Similar to the thermal conductivity gauge, the spinning rotor gauge has the best performance when the molecules can freely travel within the gauge and when the signal at the same time is significantly higher than a pressure-independent null signal. The spinning rotor gauge developed by Fremerey, [10]–[12], was the first commercially successful gauge based on the principle of gas friction. As for the thermal conductivity, the viscosity is present at all pressures, but only for pressures where the molecules freely travel within the gauge is it linearly proportional to pressure.

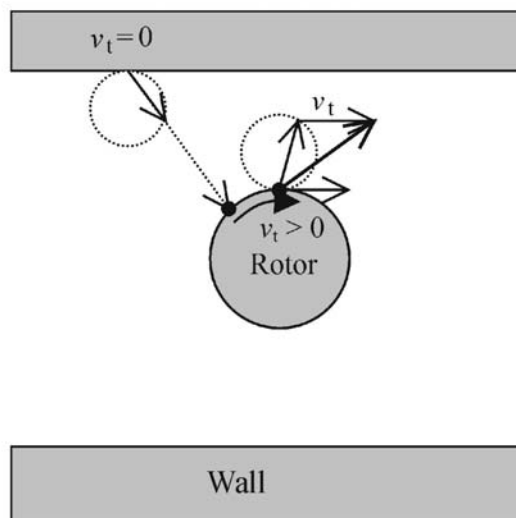


**Fig. 23:** Operating principle of the spinning rotor gauge. From *Wutz Handbuch Vakuumtechnik* by K. Jousten (ed.), Vieweg Verlag.

The operational principle of the spinning rotor gauge is shown in Fig. 23. A magnetically suspended ball of stainless steel rotates in a vacuum thimble. Molecules that hit the rotor from the wall will stick to it for a moment. If the ball did not rotate, the molecules would desorb again from it with a cosine distribution. Since the ball rotates, however, the molecules leaving the surface will have an additional velocity vector according to the tangential velocity of the rotor. The molecules will have the full tangential velocity of the rotor when they are completely accommodated to the surface. It turned out that this actually happens for technical surfaces and the accommodation factor of tangential momentum is very close to 1. This additional tangential momentum of the molecules is gained from the rotational energy of the rotor. This means that the rotor decelerates with each molecule hitting and leaving the rotor.

The whole effect can be nicely modelled and calculated and the result is that the relative deceleration rate  $\dot{\omega}/\omega$  of the rotor is proportional to pressure. Considering also a pressure-independent residual drag  $RD$ , the pressure is obtained from the measurement signal  $\dot{\omega}/\omega$  by

$$p = \sqrt{\frac{8kT}{\pi m}} \cdot \frac{\pi d \rho}{20\sigma} \left[ \left( \frac{\dot{\omega}}{\omega} \right) - RD(\omega) \right]. \quad (6)$$

Here  $T$  is the temperature,  $m$  the molecular mass,  $d$  the diameter,  $\rho$  the density of the rotor,  $\sigma$  the accommodation factor, and  $\omega$  the rotor frequency.

Figure 24 shows the schematic of a spinning rotor gauge. The weight of the rotor (1) is mainly balanced by a permanent magnet (3). Additional coils (4) on the top and the bottom suspend and stabilize the rotor vertically, four coils (8) stabilize the rotor in the two horizontal directions. The rotor is accelerated to about 415 Hz by another four coils (5) and the rotor frequency is detected by another two coils (6). They detect the rotating magnetic moment (normally a dipole) of the ball. By the generated current and also by eddy currents generated in the thimble and in the rotor itself by inhomogeneities in the magnetic field, the rotor is slowed down independent of the gas molecules impinging on it. This causes the residual drag  $RD$ .

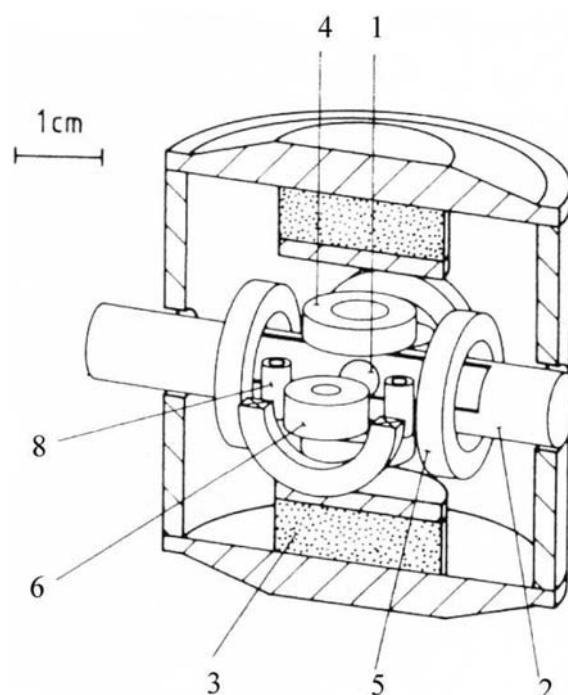


**Fig. 24:** Schematic of a spinning rotor gauge. 1 rotor; 2 vacuum tube; 3 permanent magnets; 4 two coils for vertical stabilization; 5 four drive coils; 6 two detection coils; 8 four coils for horizontal stabilization. From *Wutz Handbuch Vakuumtechnik* by K. Jousten (ed.), Vieweg Verlag.



Unfortunately this residual drag often depends on the frequency as can be seen in Fig. 25. Since the residual drag corresponds to a nitrogen pressure of  $10^{-4}$  Pa to  $10^{-3}$  Pa, pressure measurements in this range and lower need a careful evaluation of  $RD$  vs. frequency. Also a stable temperature is required since the pirouette effect by thermal expansion will slow down (or accelerate) the rotor.

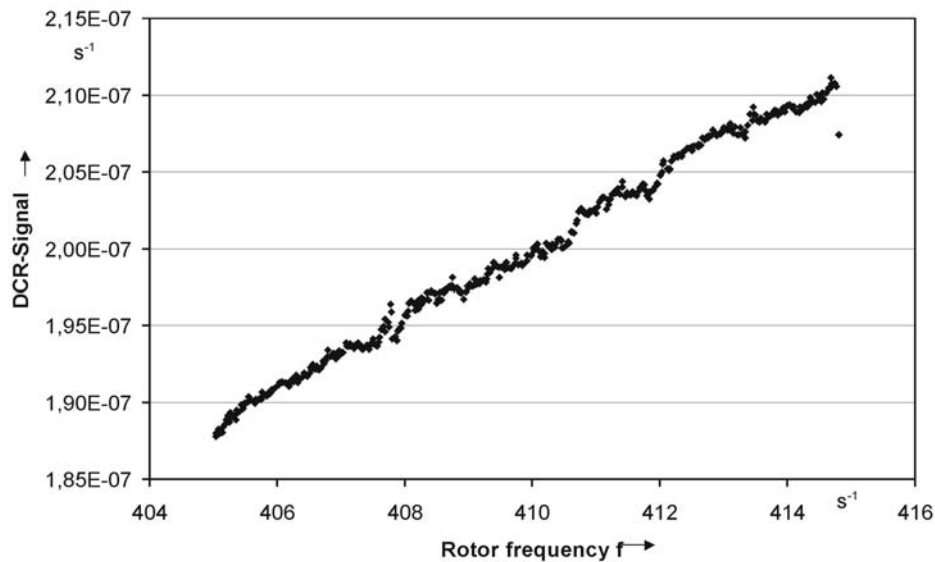


**Fig. 25:** Residual drag (DCR-signal) vs. rotor frequency for a given rotor. From *Wutz Handbuch Vakuumtechnik* by K. Jousten (ed.), Vieweg Verlag.

The measurement range of the spinning rotor gauge is from  $10^{-4}$  Pa to about 1 Pa. Lower pressures are possible with vibration isolation; at higher pressures the rotor needs frequent re-accelerations, warms up, heats the surrounding gas and the accuracy is lost. At pressures of about 100 Pa the signal becomes independent of pressure, since the gas becomes a continuum.

The spinning rotor gauge is a completely inert vacuum gauge: it does not consume any gas (e.g., by ionization); it does not dissociate molecules (like a hot cathode); its outgassing rate is the same as the thimble wall material. It is an ideal instrument to measure outgassing rates by the pressure-rise method. In addition the spinning rotor gauge gives a very accurate signal (uncertainty as low as 0.3%) and the long-term stability is excellent. For this reason it is an ideal secondary and reference standard in high vacuum and can be used to calibrate ion gauges.

### 3.3 Ionization gauges for fine vacuum

Since ionization gauges are treated in another article on UHV gauges, we restrict ourselves here to ionization gauges for higher pressures ( $> 0,1$  Pa). For the ionization principle we also refer to this article. Figure 26 gives the pressure reading obtained from the collector current for different types of ionization gauges. In all cases there is a turning point where a higher pressure causes a lower signal. There are several reasons for this.

- The mean free path of the electrons is reduced at higher pressures. With lower energy the ionization probability decreases.
- The mean free path of the ions is reduced. The collision with neutrals may reduce the probability that the ion reaches the collector.
- The secondary electron current from the ionized molecules becomes close to the primary electron current. Since the total current is kept constant, the ionization rate is reduced.

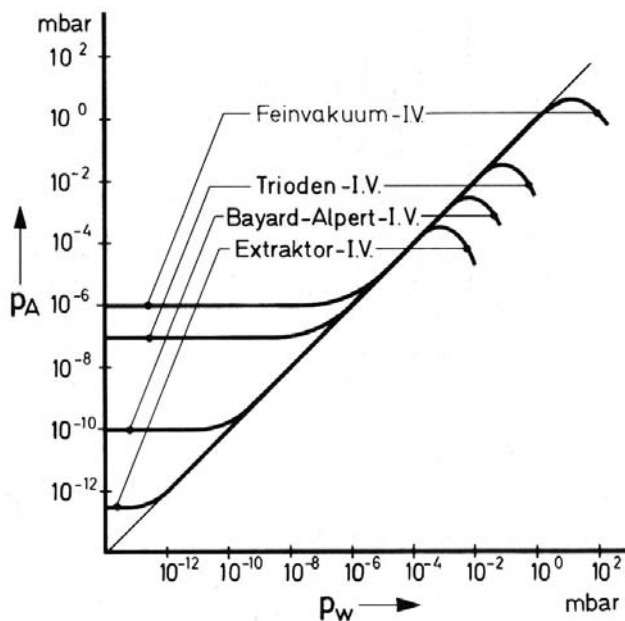


**Fig. 26:** Pressure reading obtained from the collector current vs. true pressure for different types of ionization gauges. From *Wutz Handbuch Vakuumtechnik* by K. Jousten (ed.), Vieweg Verlag.

To make an ionization gauge work at high pressures, the distances between the electrodes have to be reduced, the collector surface is enlarged, and the collector geometry must be such that the collection efficiency is optimized [13]. Figure 27 shows an example. Compared with the classical triode gauge, in the fine vacuum ionization gauge of Fig. 27 the anode and collector have changed position.

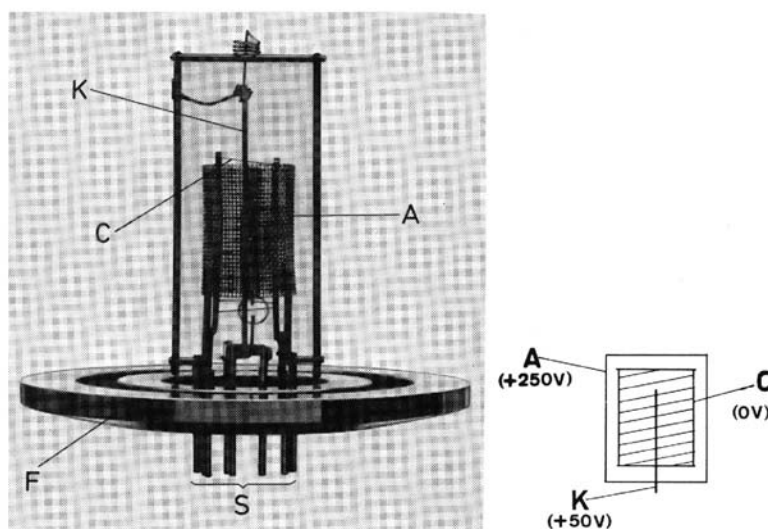


**Fig. 27:** Fine vacuum ionization gauge by Leybold Co. From *Wutz Handbuch Vakuumtechnik* by K. Jousten (ed.), Vieweg Verlag.

Last but not least, it is necessary to operate hot cathodes in ionization gauges for the fine vacuum with an oxide layer on an iridium cathode ( $\text{ThO}_2/\text{Ir}$  or  $\text{Y}_2\text{O}_3/\text{Ir}$ ) to avoid rapid ageing due to corrosion by water vapour or air components. It is also necessary to operate the gauge at a low emission current (about 0.1 mA or less).

### 3.4 Optical methods

There were a number of classical optical methods attempted in the past, but the reader is referred to textbooks (e.g., Ref. [14]), since these attempts did not have a lasting effect. For accelerators and other long vacuum systems like gravitational wave detectors, it is worth noting, however, that there were a number of successful partial pressure measurements with tunable diode laser absorption spectroscopy ([15]–[17]). For example, with an infrared (IR) laser beam of a length of 100 m a resolution of  $10^{-5}$  Pa for CO was described [15]. With multireflection cells a geometrical distance can easily be enlarged by a factor of 100 for the total path length. In long vacuum systems it seems feasible to reach resolutions in the UHV range for many IR absorbing gases like H<sub>2</sub>O, CO, CO<sub>2</sub>, CH<sub>4</sub>. Clearly, all sensitive absorption measurements are gas-species selective and it is not possible to measure a total pressure. The advantage of this kind of partial pressure measurement is that it is an inert system (no dissociation, ionization, no chemical reactions, no outgassing etc.), you can average out gas density measurement over a long path (not a point measurement as with normal vacuum gauges), and areas are accessible that are otherwise not measurable.

## 4 Accuracy of vacuum gauges

For many users the accuracy of vacuum gauges is of minor importance, since either they need the vacuum pressure information only to switch between pumps, to open and close valves etc. and work otherwise at residual pressure or, when they start a process or experiment by admitting gas into their system, they ‘calibrate’ their vacuum gauges by the success or failure of the process or experiment. While the latter procedure certainly raises some questions, the accelerator community in the routine operation belongs mainly to the first group and they need the reading of vacuum gauges with perhaps an accuracy of a factor of 2. However, when the accelerator community exchanges data like photodesorption yields, outgassing rates, cross-sectional areas, pumping speeds etc., the values should be absolute in order to be comparable and in order to be usable at different places.

Considering the last point, this concluding section will make the reader pay attention to the uncertainty of measured values with vacuum gauges as already mentioned in the introduction. It should be made clear that in general any measured value is not of much use when there is no additional value about the estimated uncertainty of this value. Only this pair (value, uncertainty) makes it possible to have confidence in a measurement and to compare results.

Table 1 lists the sources of uncertainties that may contribute in general to the total uncertainty of a measured result of a vacuum gauge. Table 2 lists the sources that are directly related to the measurement with the vacuum gauge.

**Table 1:** Sources of uncertainties that contribute to the total uncertainty of a measured result of a vacuum gauge

General	Example
Uncertainties due to calibration chain	Has the vacuum gauge been ever calibrated? Against what standard?
Uncertainties due to installation	Pressure at gauge position may not reflect the pressure where the experiment takes place.
Uncertainties due to operation	Outgassing of an ion gauge may falsify an outgassing rate measurement.
Inaccuracies caused by the physical principle of measurement	Thermal conductivity or ion gauge is used, but gas mixture is not (accurately) known.
Uncertainties caused by the device itself	See Table 2.

**Table 2:** Sources of uncertainties due to the vacuum gauge itself

General	Examples
Offset measurement	Residual drag in SRG, zeroing of Pirani gauge, X-ray and ESD effect for ion gauges
Offset instability (drift)	Offset drifts with environmental temperature (pirouette effect in SRG), bridge is no more balanced with time
Resolution	Number of digits shown
Influence of environment (mainly temperature)	Enclosure temperature of Pirani changes, varies, thermal transpiration effect changes in CDG, amplifier changes amplification
Non-linearity	Ion gauge (sensitivity changes with pressure)
Integration time (scatter of data), repeatability	Same signal at repeat measurements? Integration time in SRG, in picoammeter with ion gauge.
Reproducibility (stability of calibration constant)	Calibration constants change with time.
Hysteresis	Mechanical gauges (up, down measurement)
Prior usage, cleanliness	Surfaces change, accommodation coefficients change, secondary yield changes

A typical problem of uncertainty is the use of an indirectly measuring vacuum gauge whose reading is gas-species dependent but the composition of the measured gas is not known. In this case, most people use the trick to give the value ‘pressure as nitrogen equivalent’. This means that the gauge is calibrated or set to nitrogen and the reading is taken as nitrogen equivalent pressure. The true pressure of the real gas composition may be far different.

If the gas composition is approximately known (uncertainty!), very often a weighted mean may be taken to correct for a true pressure reading. For example, for the spinning rotor gauge an effective mass

$$m_{\text{eff}} = \left( \sum_{i=1}^n a_i \sqrt{m_i} \right)^2 \quad \sum_{i=1}^n a_i = 1 \quad (7)$$

can be used, where  $a_i$  is the relative portion of molecule  $m_i$  of the total pressure with  $n$  components [18]. Similarly, the correction factors  $CF$  for gas species can be taken for thermal conductivity gauges or ion gauges:

$$CF_{\text{eff}} = \sum_{i=1}^n a_i CF_i \quad (8)$$

Table 3 lists the total measurement range, the typical relative uncertainty in this range, the optimum measurement range, and the relative measurement uncertainty in the latter for several commercial vacuum gauges including gauges for the UHV. ‘Relative’ means compared to the indicated value. Figure 28 illustrates this table graphically, but also the uncertainties of the vacuum pressure scale as realized by the three primary standards (mercury manometer, static expansion, and continuous expansion [19]) are given.

**Table 3:** Relative measurement uncertainty of commercially available vacuum gauges

Gauge type	Measurement range in Pa	Normal uncertainty	Optimum range in Pa	Lowest uncertainty
Piston gauge	$10^{-10}$ – $10^5$		$10^2$ – $10^5$	$1 \cdot 10^{-4}$ – $1 \cdot 10^{-5}$
Quartz Bourdon manometer	$10^3$ – $10^5$		$10^3$ – $10^5$	$3 \cdot 10^{-4}$ – $2 \cdot 10^{-4}$
Resonance silicon gauge	$10^{-10}$ – $10^5$	$3 \cdot 10^{-3}$ – $5 \cdot 10^{-4}$	$100$ – $10^5$	$2 \cdot 10^{-4}$ – $5 \cdot 10^{-5}$
Mechanical vacuum gauge	$10^2$ – $10^5$	0.1–0.01		
Membrane vacuum gauge	$10^2$ – $10^5$	0.1–0.01		
Piezo	$10^2$ – $10^5$	1–0.01		
Thermocouple gauge	$10^{-1}$ – $10^2$	1–0.3		
Pirani gauge	$10^{-1}$ – $10^5$	1–0.15	1–100	0.1–0.05
Capacitance diaphragm gauge	$10^{-4}$ – $10^5$	$10^{-1}$ – $3 \cdot 10^{-3}$	$10^{-1}$ – $10^5$	$4 \cdot 10^{-3}$ – $1 \cdot 10^{-3}$
Spinning rotor gauge	$10^{-5}$ – $10$	0.1– $7 \cdot 10^{-3}$	$10^{-3}$ – $10^{-1}$	$4 \cdot 10^{-3}$
Penning gauge	$10^{-7}$ – $1$	$5 \cdot 10^{-1}$ – $2 \cdot 10^{-1}$	$10^{-5}$ – $1$	$3 \cdot 10^{-1}$ – $1 \cdot 10^{-1}$
Magnetron gauge	$10^{-8}$ – $1$	1– $1 \cdot 10^{-1}$	$10^{-6}$ – $1$	$1 \cdot 10^{-1}$ – $2 \cdot 10^{-2}$
Ionization gauge (emission cathodes)	$10^{-10}$ – $10^{-2}$	$1.5 \cdot 10^{-1}$ – $5 \cdot 10^{-2}$	$10^{-8}$ – $10^{-2}$	$5 \cdot 10^{-2}$ – $2 \cdot 10^{-2}$

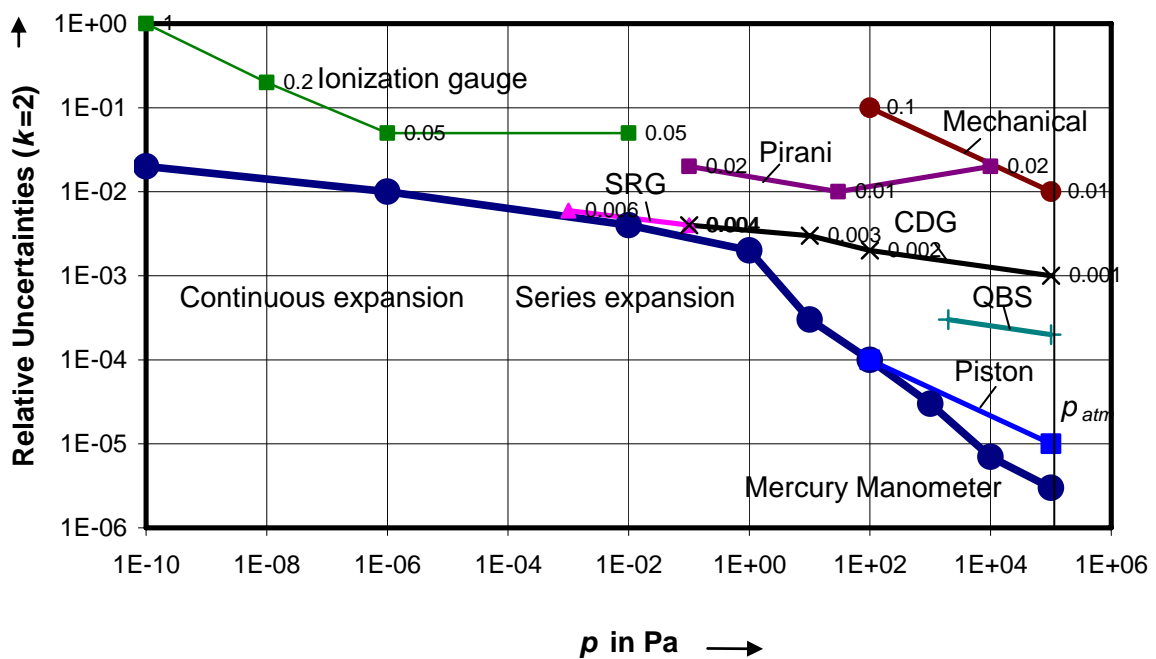


**Fig. 28:** Illustration of the relative uncertainties of the vacuum pressure scale by primary standards (bold line) and commercially available vacuum gauges

## References

- [1] <http://www.bipm.org>
- [2] S. J. Bennet, P. B. Clapham, J. E. Dadson and D. I. Simpson, Laser interferometry applied to mercury surfaces, *J. Phys. E: Sci. Instrum.* **8** (1975) 5–7.
- [3] J. Jäger, Use of a precision mercury manometer with capacitance sensing of menisci, *Metrologia* **30** (1993/94) 553–558.
- [4] P. L. Heydemann, A fringe-counting pulsed ultrasonic interferometer, *Rev. Sci. Instrum.* **42** (1971) 983–986.
- [5] J. J. Sullivan, Development of variable capacitance pressure transducers for vacuum applications, *J. Vac. Sci. Technol. A* **3** (1985) 1721–1730.
- [6] K. Harada, Various applications of resonant pressure sensor chip based on 3-D micromachining, *Sensors and Actuators A* **73** (1999) 261–266.
- [7] T. Takaishi and Y. Sensui, *Trans. Faraday Soc.* **59** (1963) 2503–2514.
- [8] J. Setina, *Metrologia* **36** (1999) 623–626.
- [9] M. Pirani, *Deutsche Phys. Gesellschaft, Verh.* **8** (1906) 686.
- [10] J. K. Fremerey, *Rev. Sci. Instrum.* **44** (1973) 1396–1397.
- [11] J. K. Fremerey, *Vacuum* **32** (1982) 685–690.
- [12] J. K. Fremerey, *J. Vac. Sci. Technol. A* **3** (1985) 1715–1720.
- [13] G. J. Schulz and A. V. Phelps, *Rev. Sci. Instrum.* **28** (1957) 1051.
- [14] A. Berman, *Total Pressure Measurements in Vacuum Technology* (Academic Press, Orlando, FL, 1985), p.156.
- [15] E. Lanzinger, K. Jousten and M. Kühne, *Vacuum* **51** (1998) 47–51.
- [16] R. S. Inman and J. F. McAndrew, *Anal. Chem.* **66** (1994) 247–2479J.
- [17] G. J. Padilla Viquez, Dissertation, TU Berlin (2005).
- [18] L. D. Hinkle and P. R. Jacobs, *J. Vac. Sci. Technol. A* **11** (1993) 261–263.
- [19] J. M. Lafferty, *Foundations of Vacuum Science and Technology* (John Wiley and Sons, New York, 1998), Chapter 12.

## Bibliography

- A. Berman, *Total Pressure Measurements in Vacuum Technology* (Academic Press, Orlando, FL, 1985).
- Saul Dushman, *Scientific Foundations of Vacuum Technique*, 2nd edition (John Wiley & Sons, New York, 1962).
- Karl Jousten, *Wutz Handbuch Vakuumtechnik*, 9<sup>th</sup> edition (Vieweg, Wiesbaden, 2006), ISBN 3-8348-0133-X.
- James M. Lafferty, *Foundations of Vacuum Science and Technology* (John Wiley & Sons, New York, 1998).
- J.H. Leck, *Total and Partial Pressure Measurement in Vacuum Systems* (Blackie, Glasgow, 1989).
- P.A. Redhead, J.P. Hobson and E.V. Kornelsen, *The Physical Basis of Ultrahigh Vacuum* (Chapman and Hall Ltd, London, 1968). This book has recently been re-edited by the American Vacuum Society.